

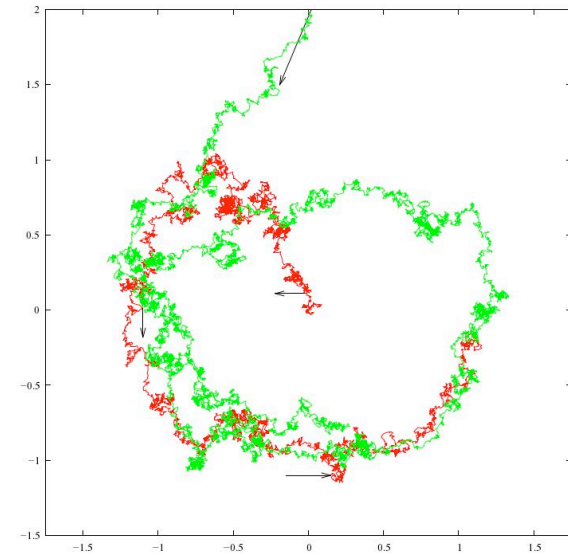
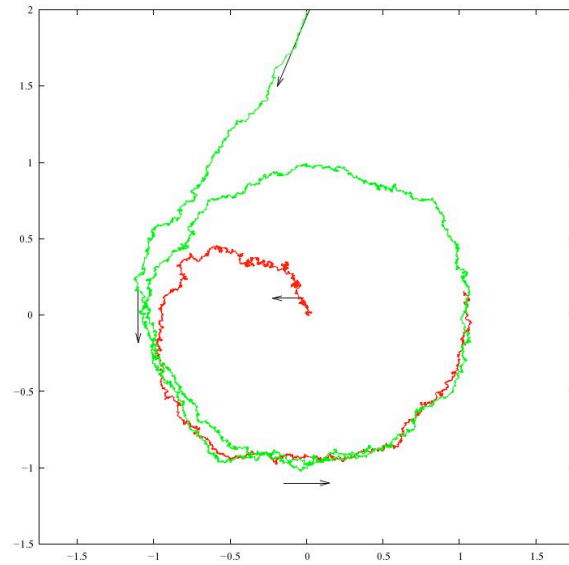
Jonathan Rubin

AIM Workshop
February 22, 2012

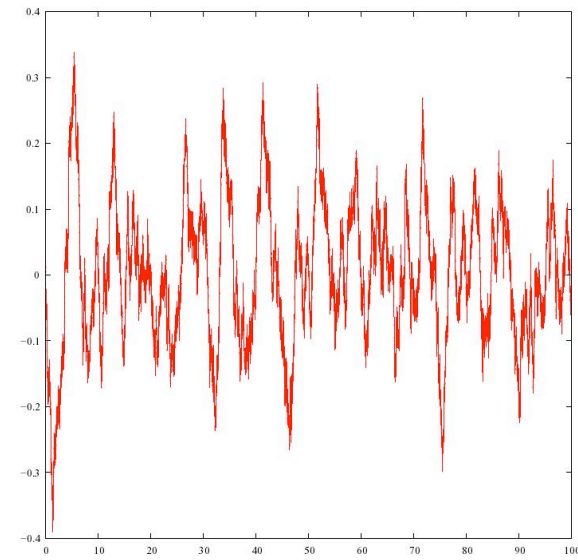
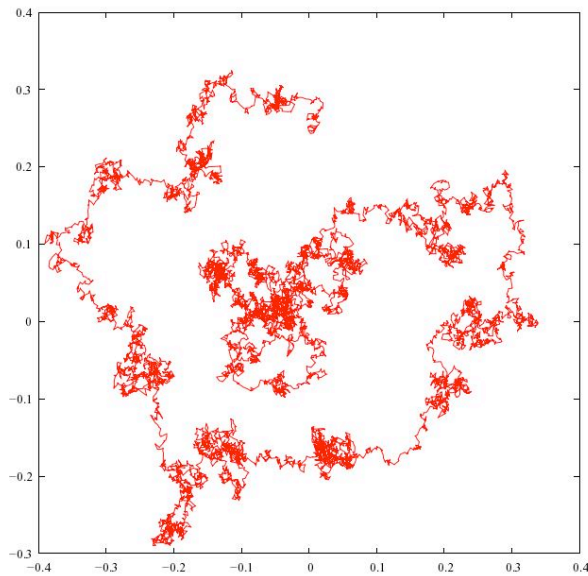
Normal Forms

noise in an Andronov-Hopf bifurcation (Azimuth Project)

with limit cycle



w/o limit cycle



theta/SNIC model

Gutkin & Ermentrout, *Neural Comp*, 1998: add comparable noise to theta model vs. AH model \Rightarrow theta model CV is twice as large

Ritt, *Phys. Rev. E*, 2003: entrainment of theta model to white noise stimulus

Planar Models

planar model – active phase as single spike

A. Bose et al. / Physica D 140 (2000) 69–94

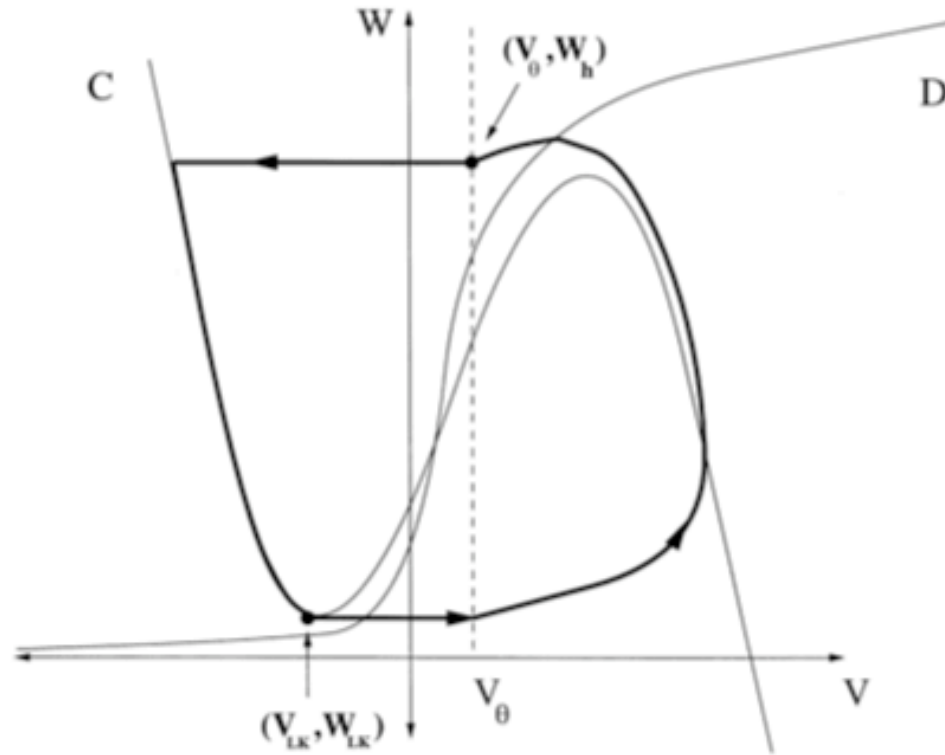


Fig. 2. The singular periodic orbit.

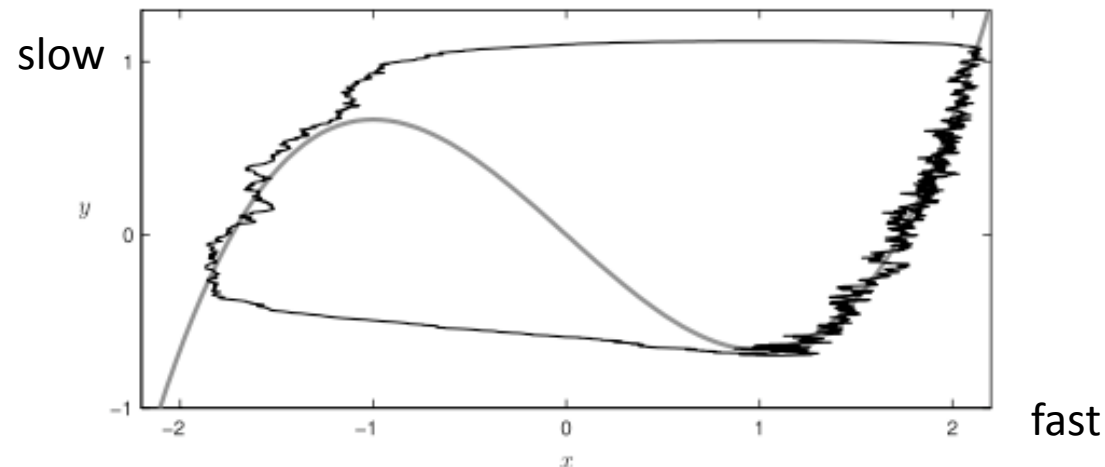
A mathematical framework for critical transitions: Bifurcations, fast-slow systems and stochastic dynamics

Christian Kuehn

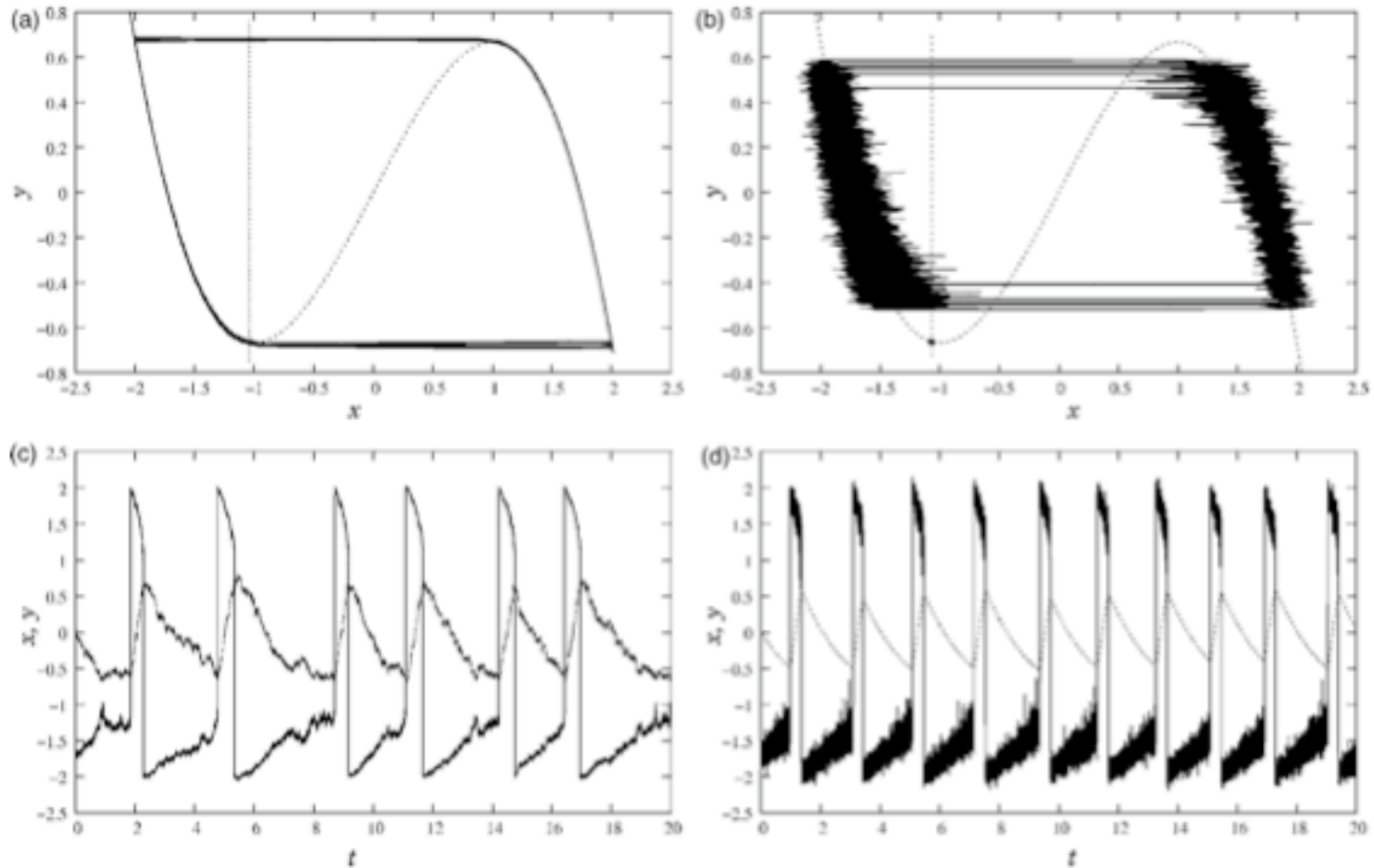
Center for Applied Mathematics, Cornell University, United States

$$\begin{aligned} dx_\tau &= \frac{1}{\epsilon}(y - x^2)d\tau + \frac{\sigma}{\sqrt{\epsilon}}dW_\tau, \\ dy_\tau &= g(x_\tau, y_\tau)d\tau, \end{aligned} \tag{34}$$

Theorem 6.1. Consider the SDE (34) and suppose $g \equiv 1$. If $\sigma \ll \sqrt{\epsilon}$ then critical transitions before the deterministic fold bifurcation point occur with very small probability. For $\sigma \gg \sqrt{\epsilon}$ critical transitions before the deterministic fold bifurcation occur with very high probability.



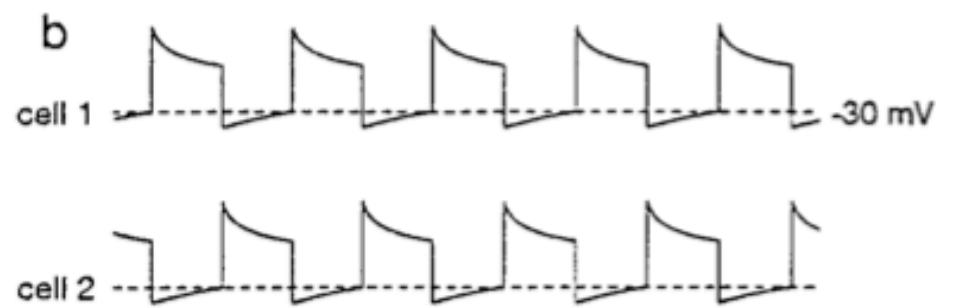
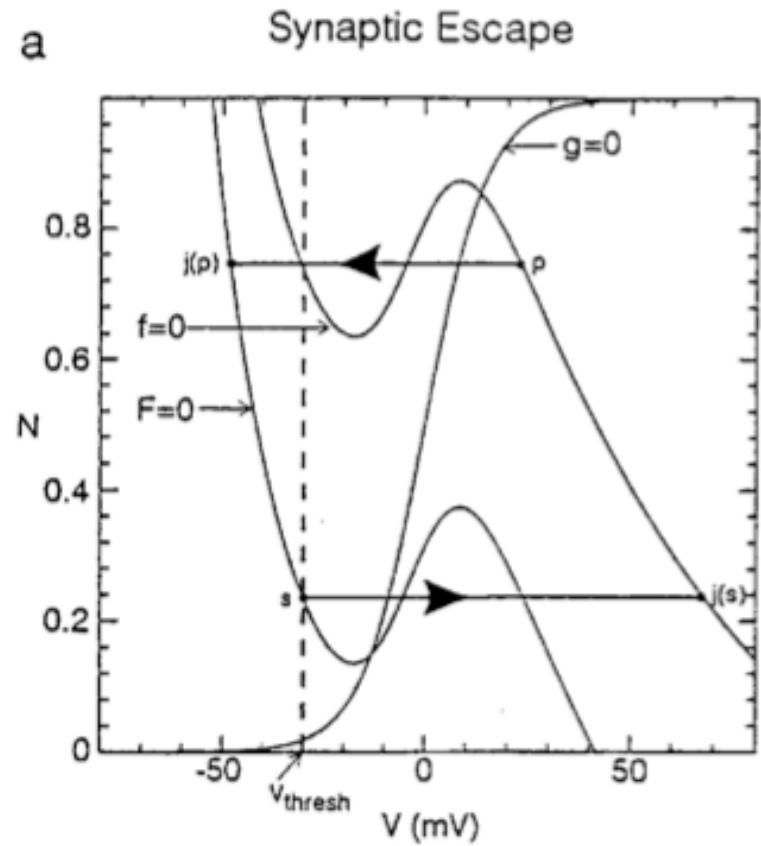
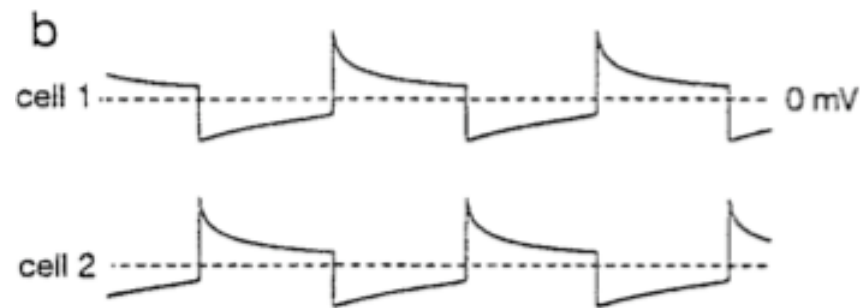
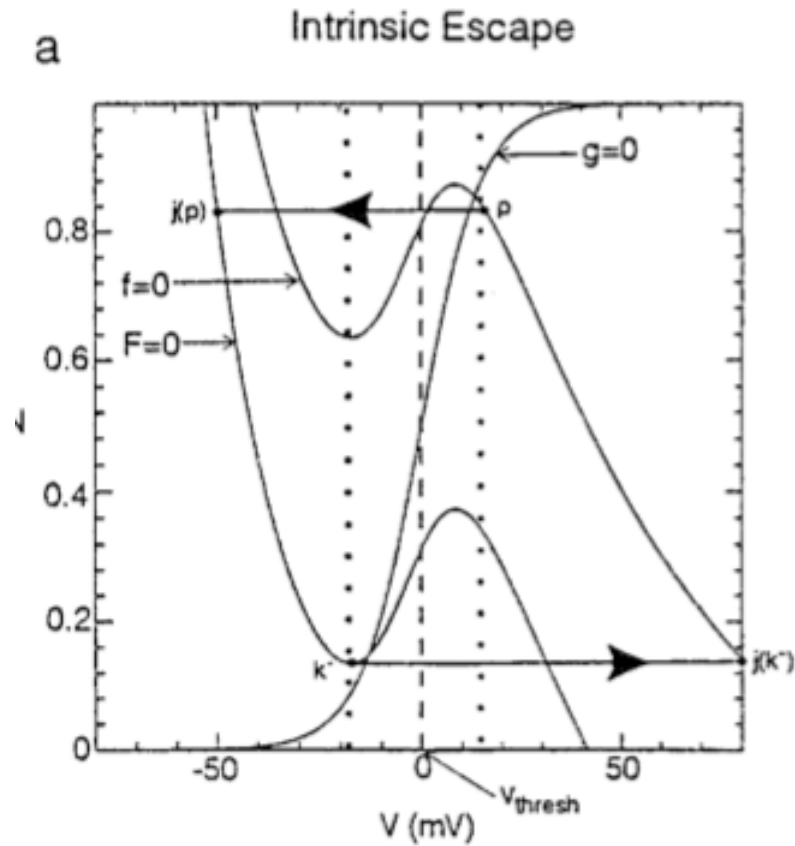
coherence resonance vs. self-induced stochastic resonance
DeVille et al., *Phys. Rev. E*, 2005



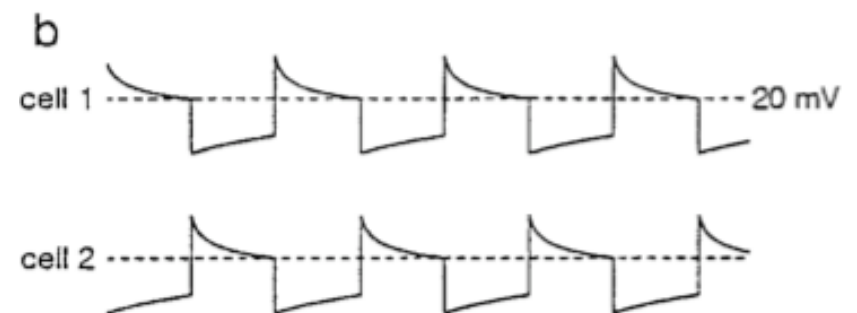
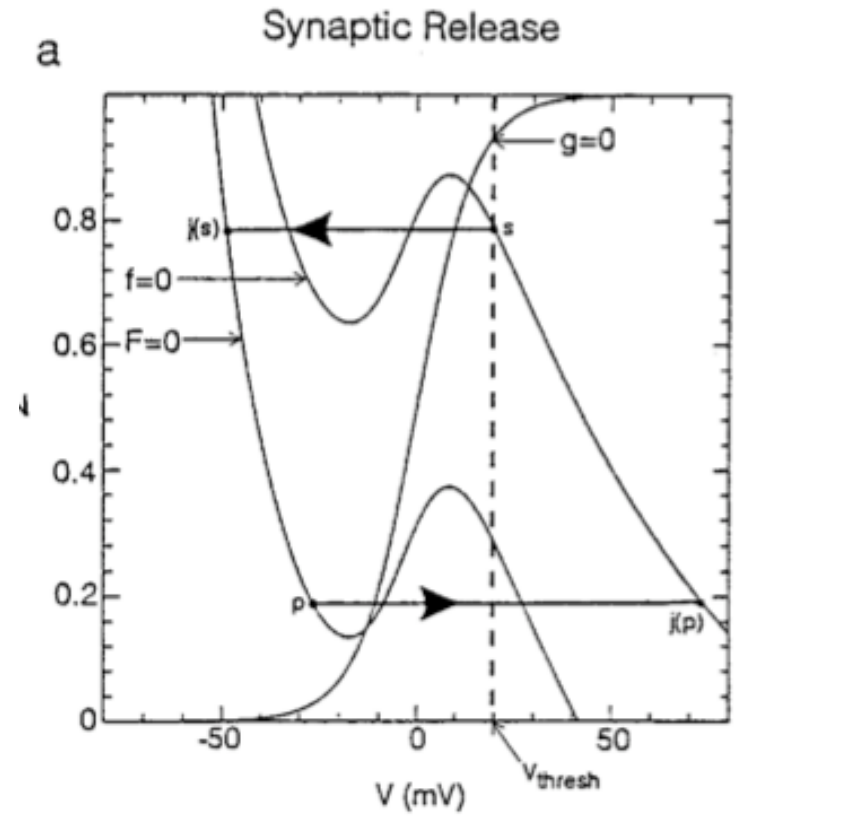
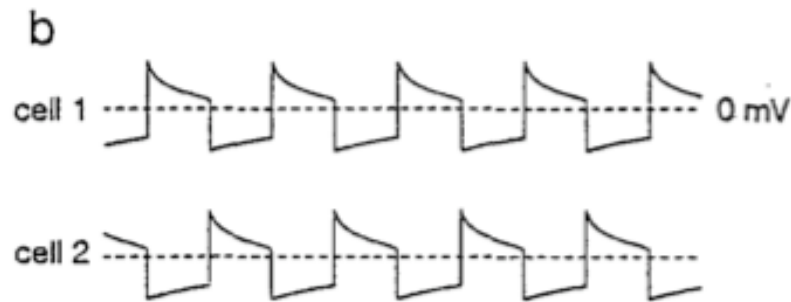
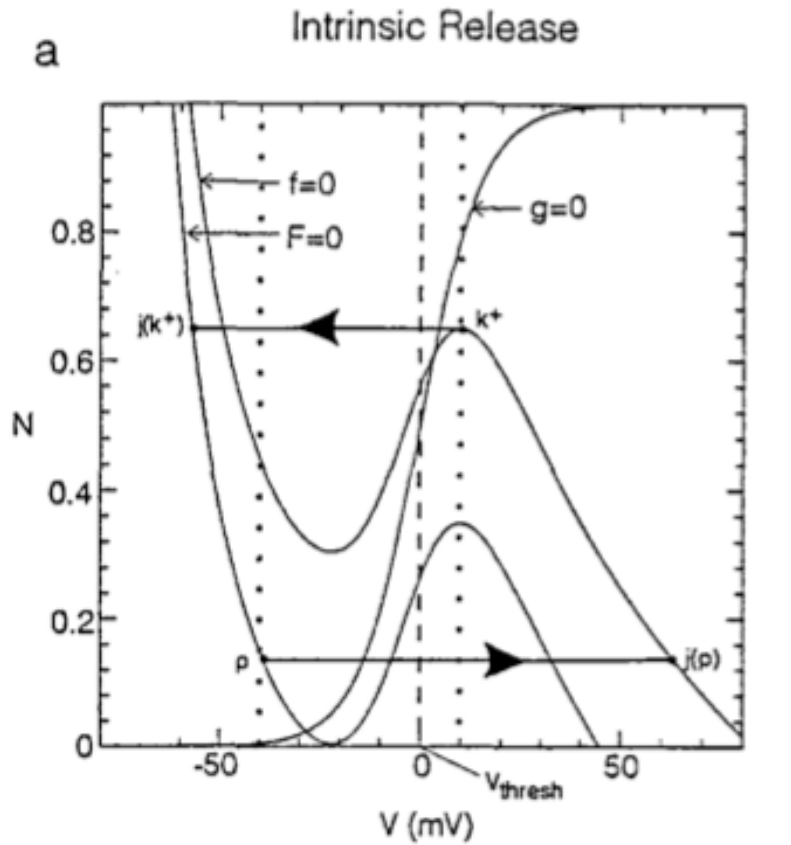
noise in slow variable

noise in fast variable

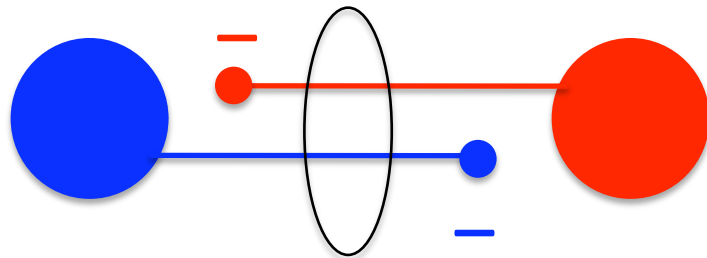
coupling between planar models – escape (Skinner et al., *JCNS*, 1994)



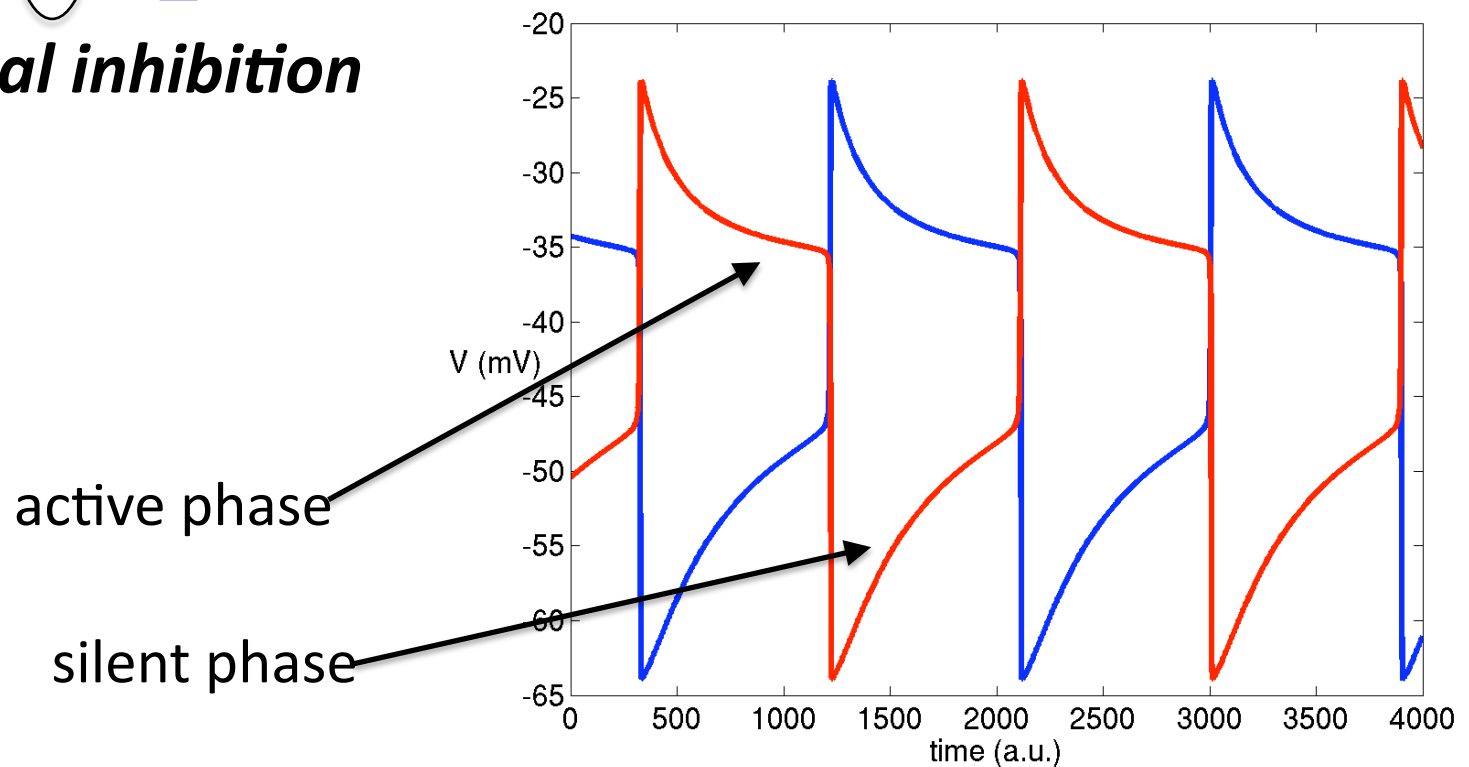
coupling between planar models – release (Skinner et al., *JCNS*, 1994)



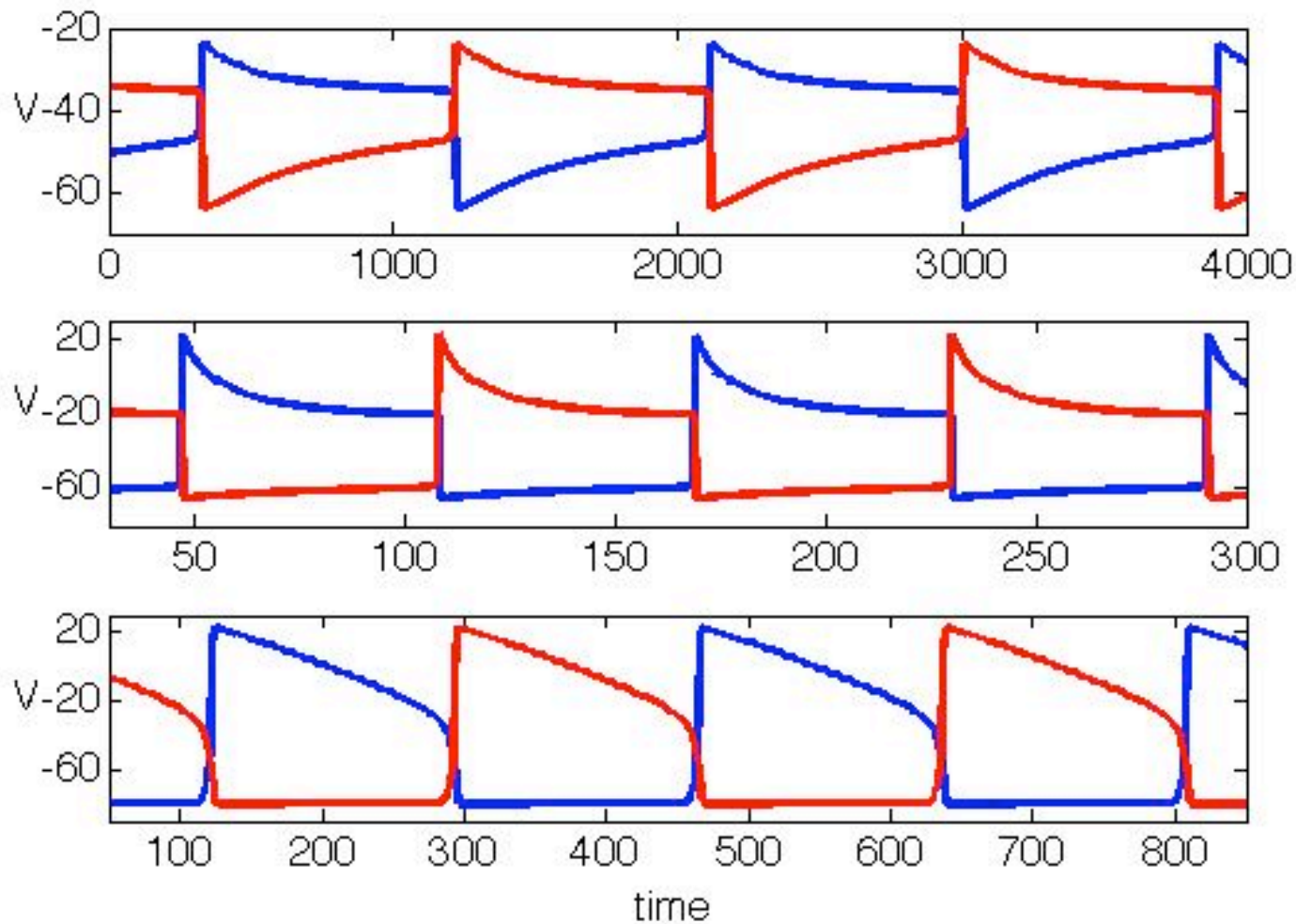
half-center oscillator (Brown, 1911): components *not intrinsically rhythmic*; generates rhythmic activity, without rhythmic drive



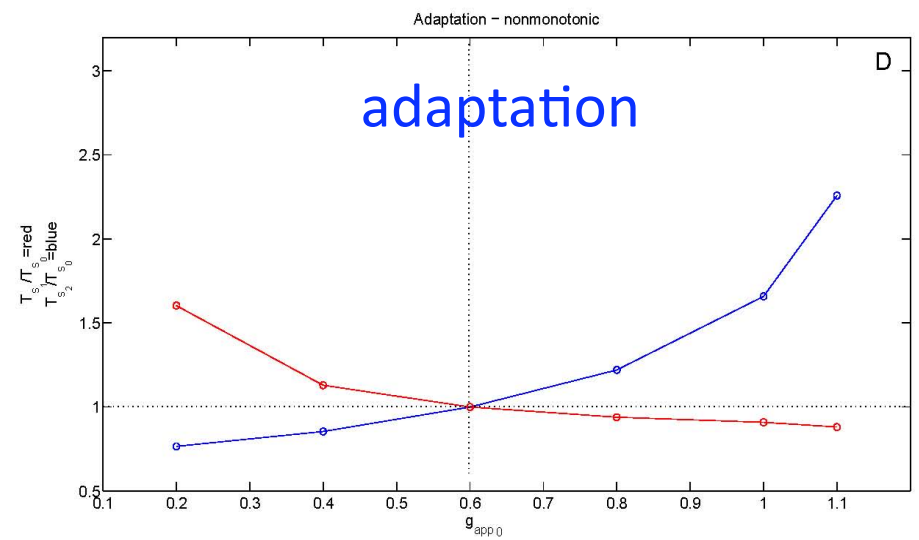
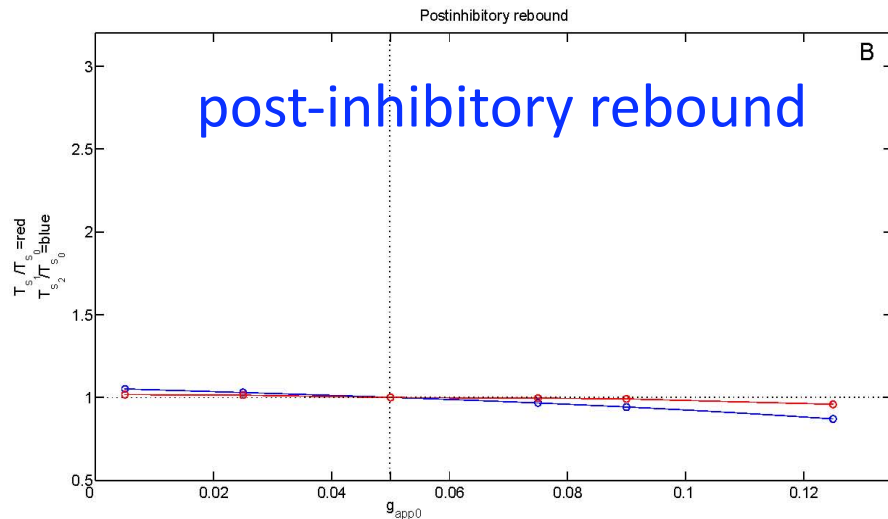
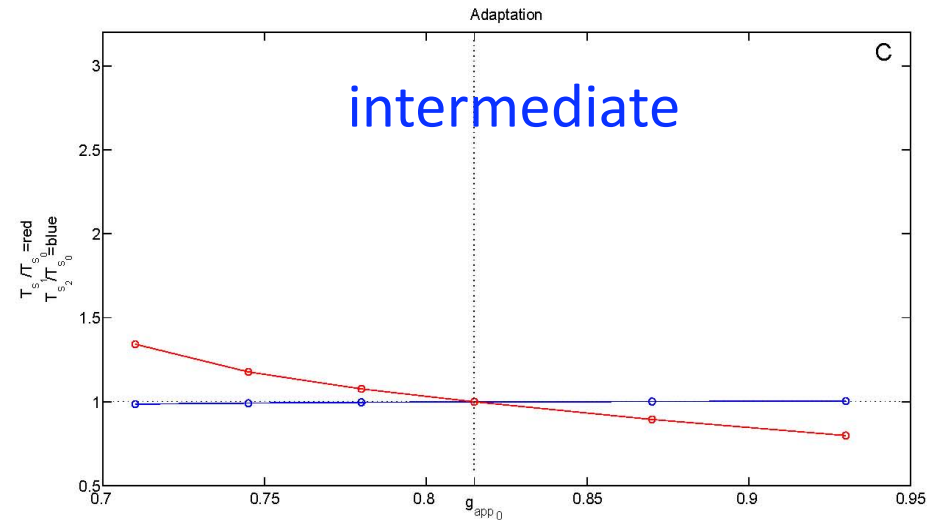
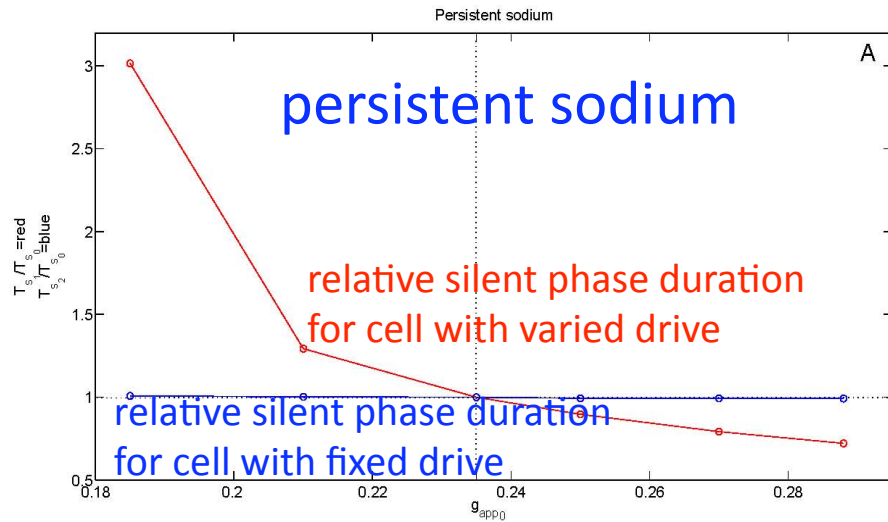
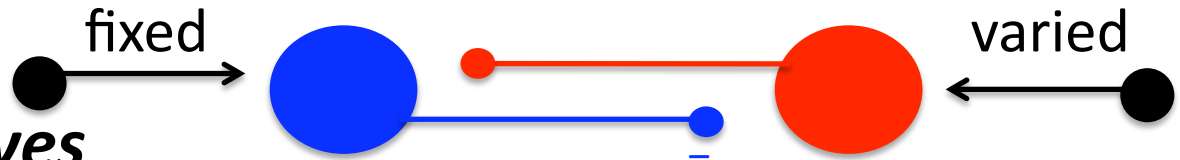
reciprocal inhibition



time courses for half-center oscillations from 3 mechanisms:
persistent sodium, post-inhibitory rebound (T-current), adaptation (Ca/K-Ca)



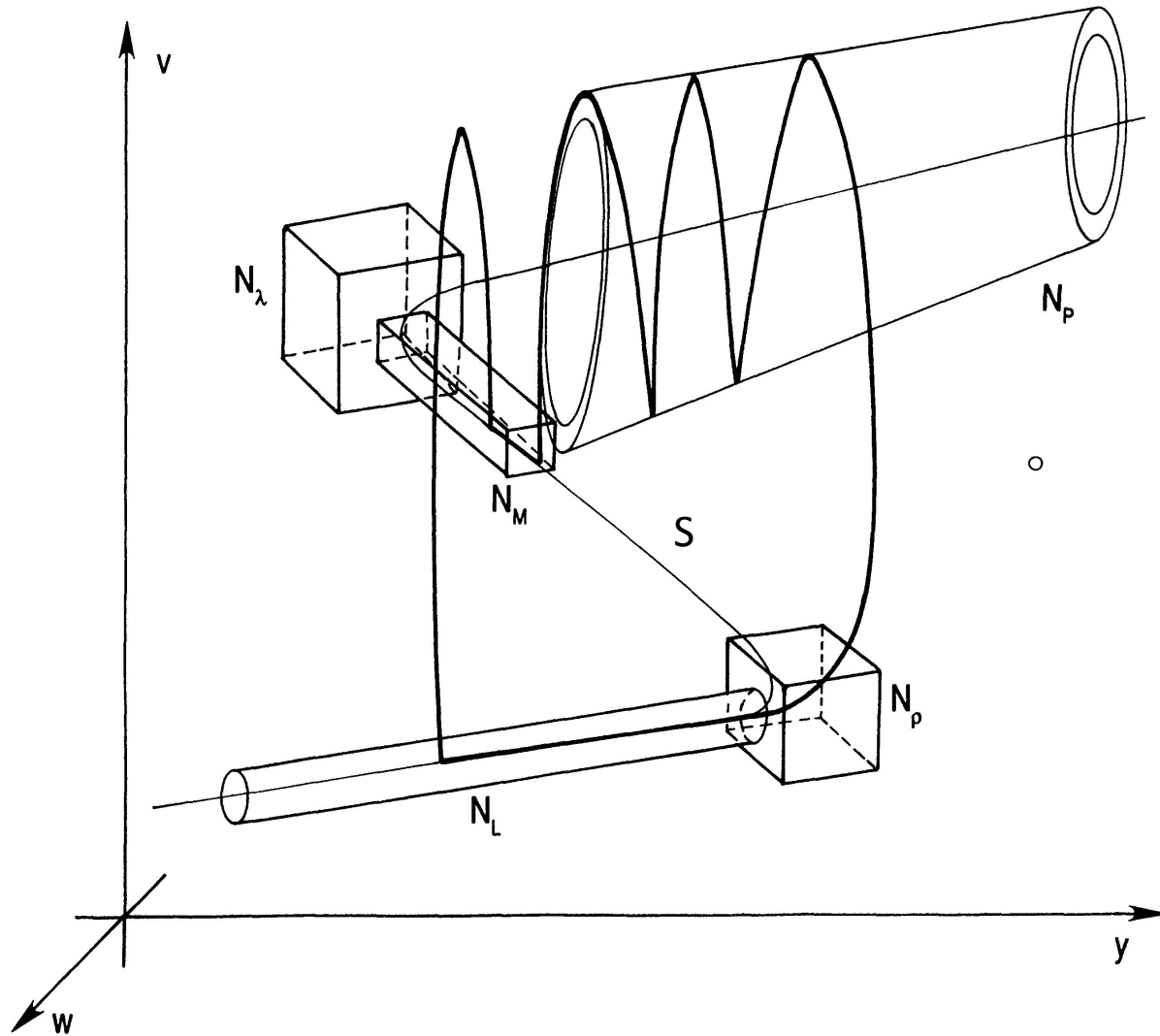
simulation results:
unequal constant drives



Daun, Rubin, and Rybak, *JCNS*, 2009

Bursting

rigorous framework for bursting – Terman, 1991-2

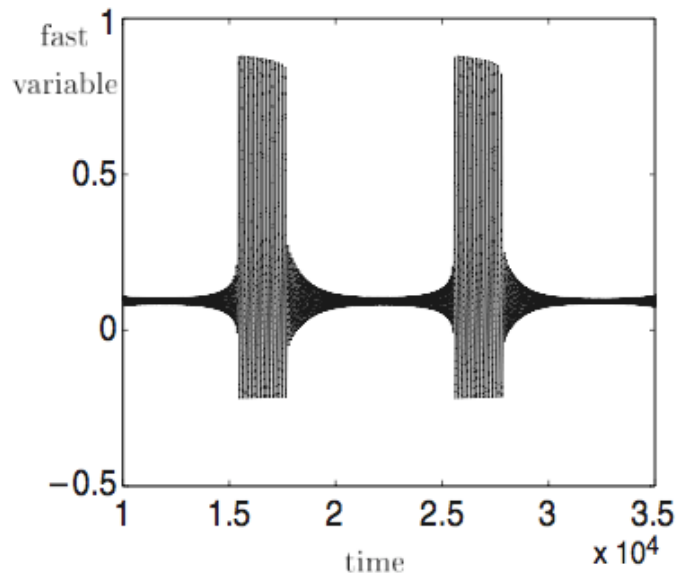


noise in bursting (example)

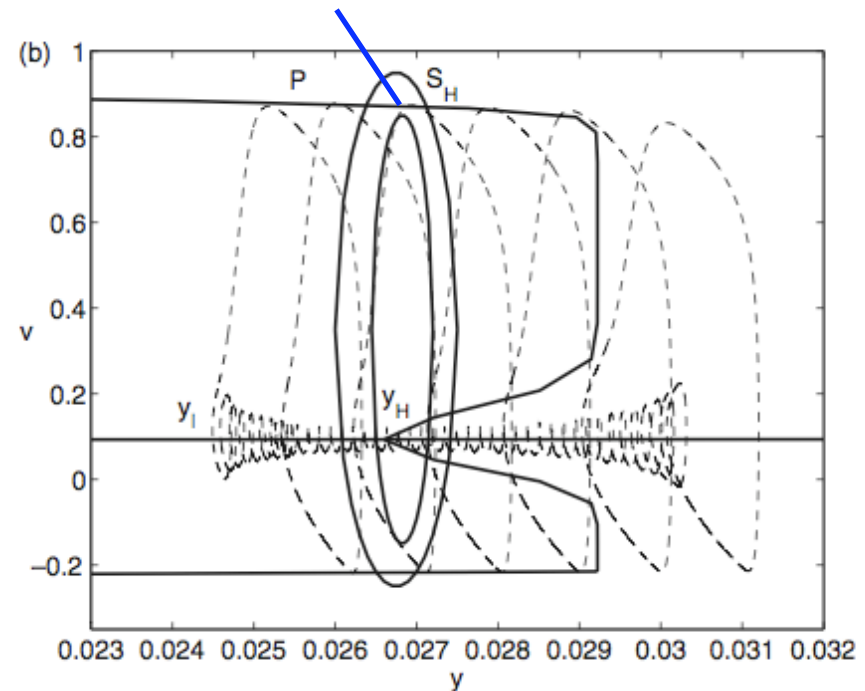
elliptic (subAH-SNPO) bursting:

Su, R. and Terman, *Nonlinearity*, 2004

section of invariant tube



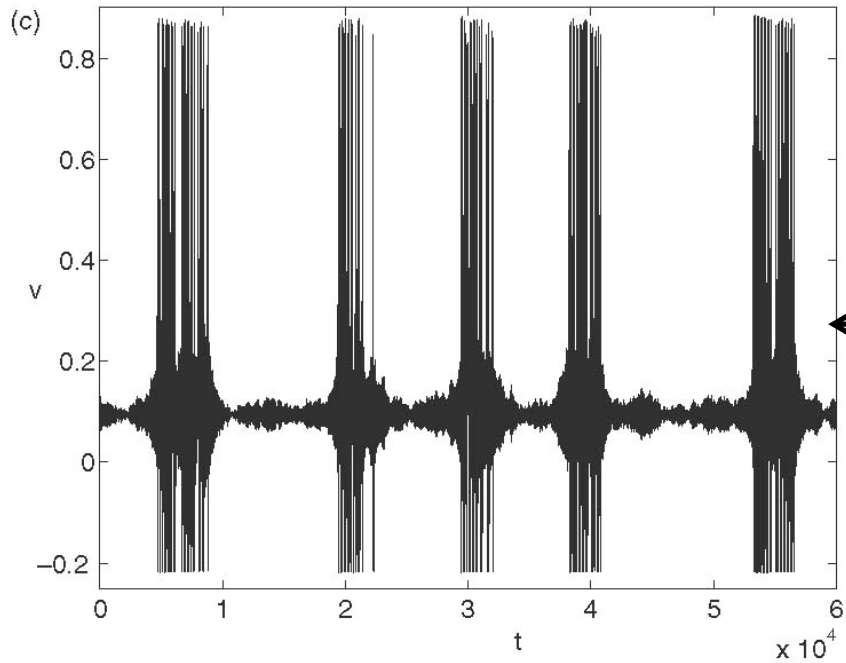
Kuske & Baer, *BMB*, 2002



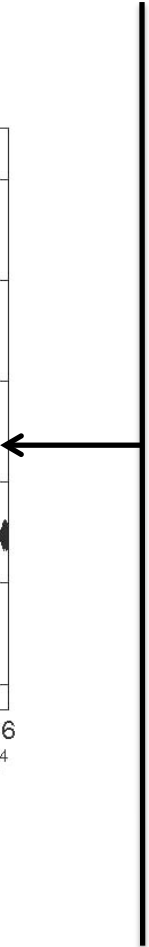
$$\begin{aligned}v' &= f_1(v, w, y) \\w' &= f_2(v, w, y) \\y' &= \varepsilon g(v, w, y), \quad 0 < \varepsilon \ll 1\end{aligned}$$

- existence of invariant tube
- estimate of passage time
- metastability of solutions

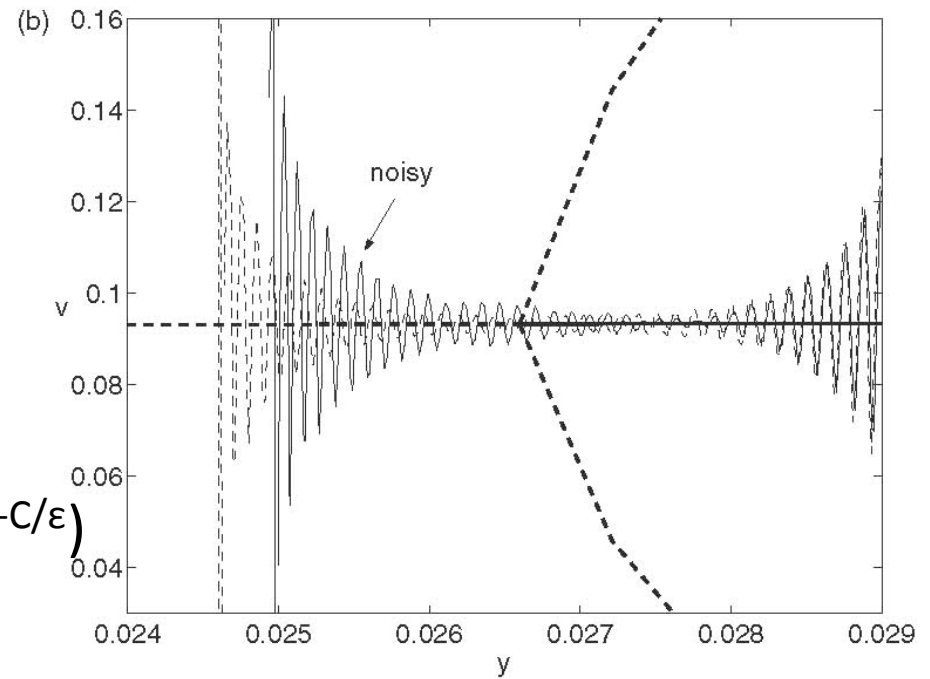
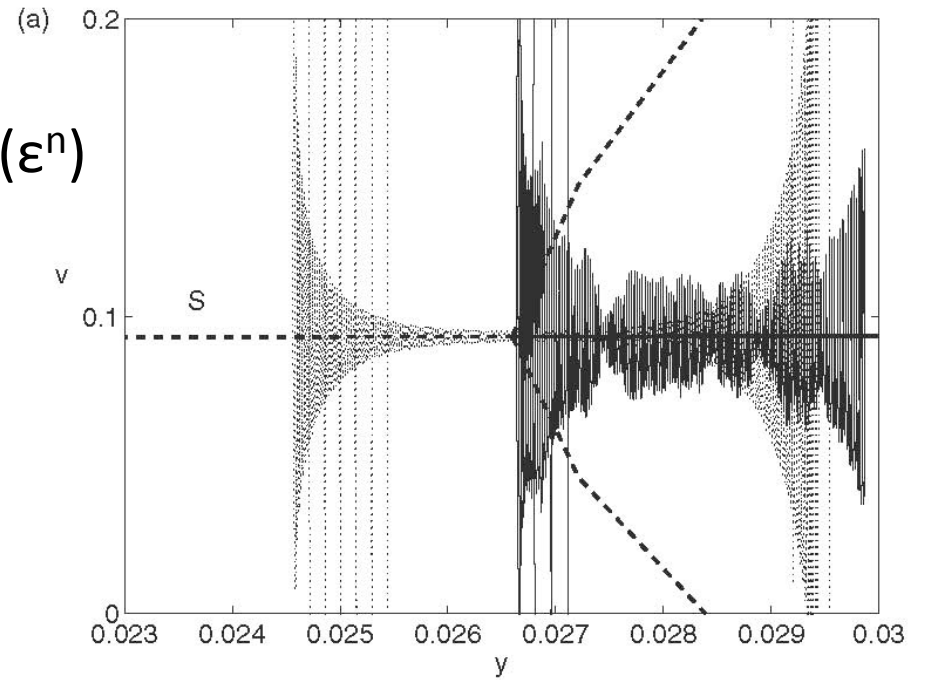
introduce noise σ



$$\sigma = O(\epsilon^n)$$



$$\sigma = O(e^{-C/\epsilon})$$



Su, R. and Terman,
Nonlinearity, 2004

A mathematical framework for critical transitions: Bifurcations, fast–slow systems and stochastic dynamics

Physica D 240 (2011) 1020–1035

Christian Kuehn

Center for Applied Mathematics, Cornell University, United States

$$\begin{aligned}dx_\tau &= \frac{1}{\epsilon} f(x_\tau, y_\tau) d\tau + \frac{\sigma_f}{\sqrt{\epsilon}} dW_\tau, \\dy_\tau &= g(x_\tau, y_\tau) d\tau + \sigma_g dW_\tau, \\(\sigma_f^2 + \sigma_g^2)^{1/2} &= \sigma = \sigma(\epsilon)\end{aligned}$$

The first goal is an estimate on the concentration of solutions to (16) near the deterministic slow manifold. To identify a neighborhood containing most sample paths we define the process

$$\xi_\tau := x_\tau - h_\epsilon(y_\tau). \tag{17}$$

Then define $X_\tau := \sigma_f^{-2} \text{Var}(\xi_\tau^0)$ which satisfies a fast-slow ODE [32] given by

$$\begin{aligned} \epsilon \dot{X} &= 2A_\epsilon(y)X + 1, \\ \dot{y} &= g(h_\epsilon(y), y). \end{aligned} \tag{20}$$

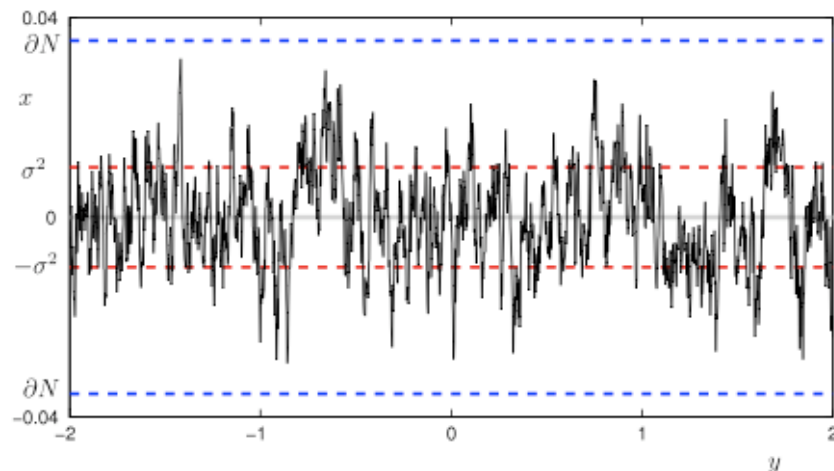
The slow manifold of (20) is

$$C_\epsilon^X = \left\{ (X, y) \in \mathbb{R}^2 : x = H_\epsilon(y) = -\frac{1}{2A_\epsilon(y)} + O(\epsilon) \right\}.$$

The neighborhood of C_ϵ is then defined as

$$N(r; C_\epsilon) := \left\{ (x, y) \in \mathbb{R}^2 : \frac{(x - h_\epsilon(y))^2}{H_\epsilon(y)} < r^2 \right\}. \tag{21}$$

Theorem 4.1. *Sample paths starting on C_ϵ stay in $N(r; C_\epsilon)$ with high probability for times approximately given by $O(\epsilon e^{r^2/(2\sigma_f^2)})$.*

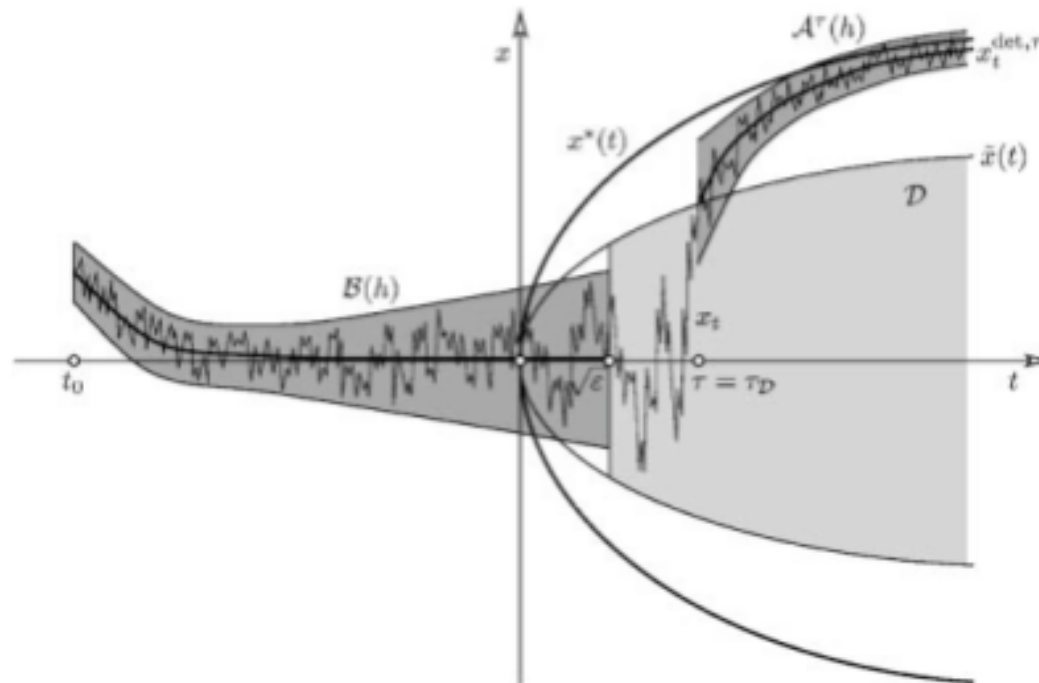


Nils Berglund · Barbara Gentz

Pathwise description of dynamic pitchfork bifurcations with additive noise

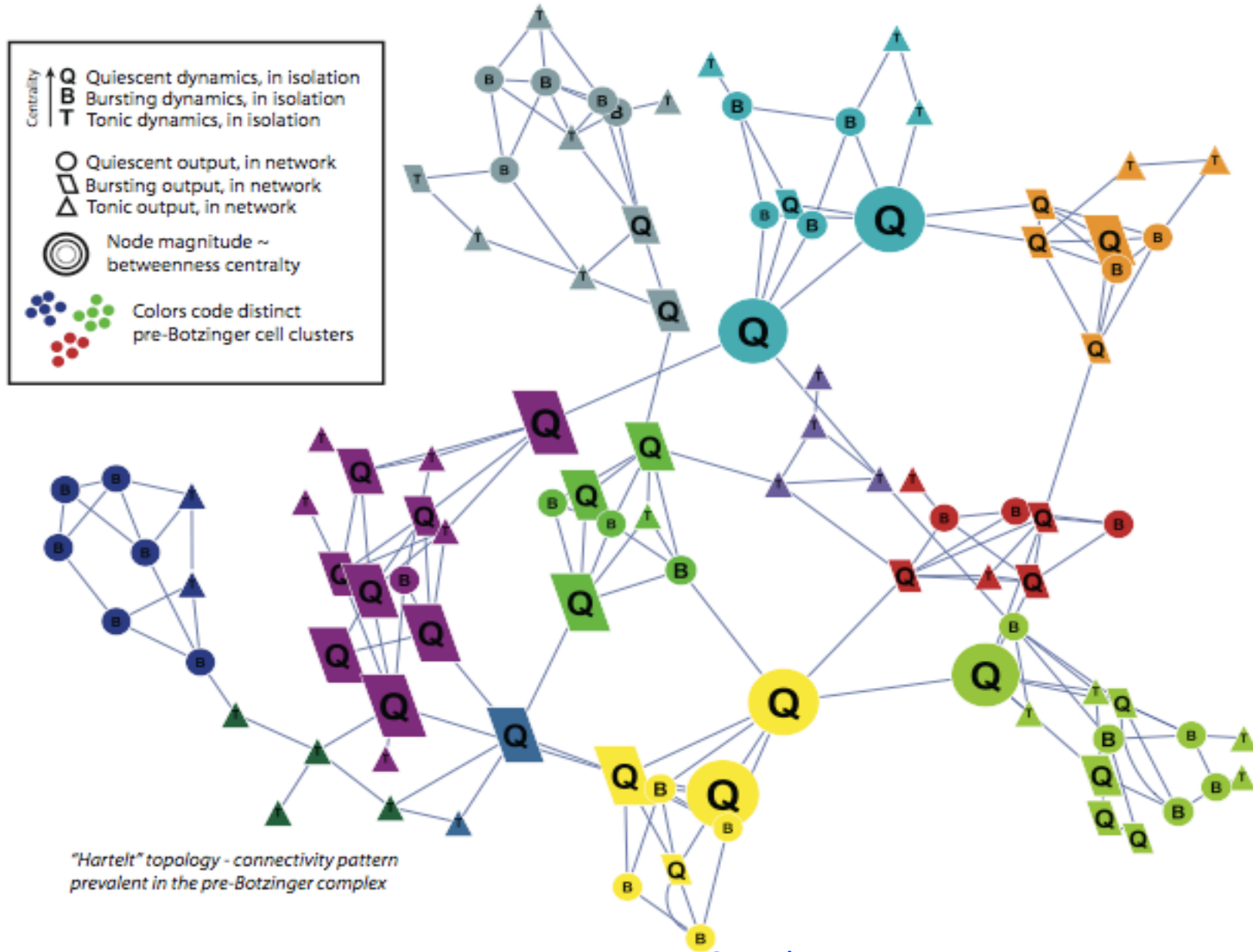
$$dx_t = \frac{1}{\varepsilon} f(x_t, t) dt + \frac{\sigma}{\sqrt{\varepsilon}} dW_t.$$

small



Network Architecture + Dynamics

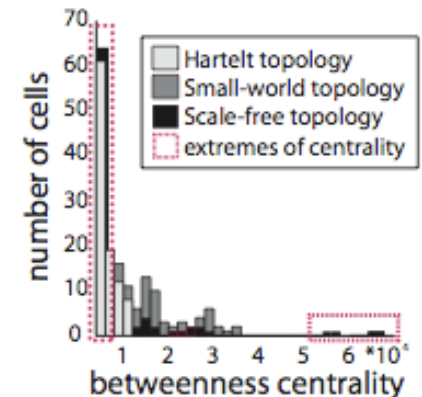
example Hartelt network – how can this synchronize?



larger network simulation study

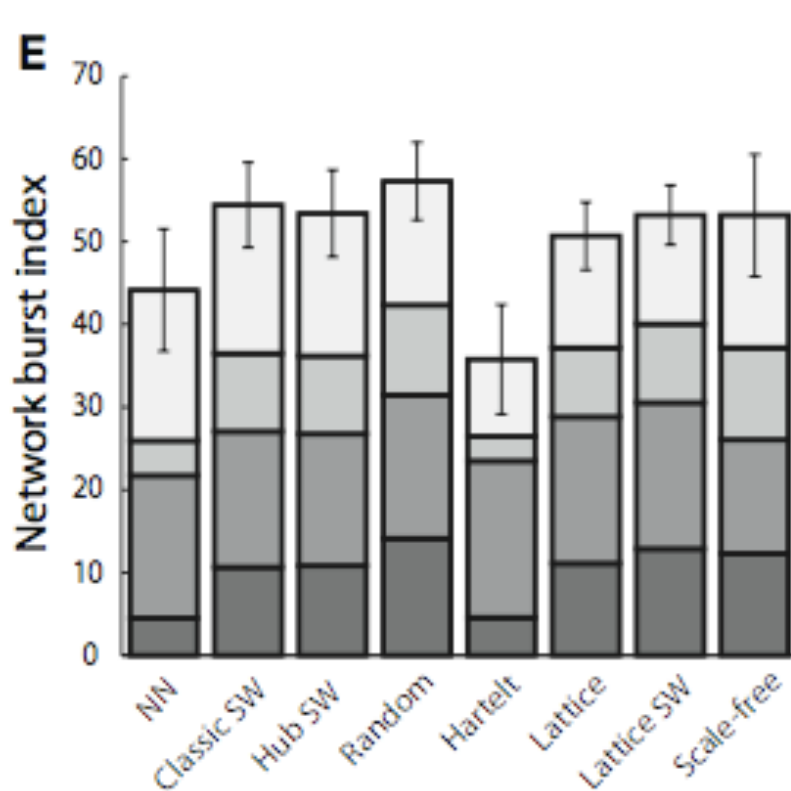
Gaiteri & Rubin, *Frontiers in Comp. Neurosci.*, 2011

- 100 square-wave bursting neurons, 90 sec/sim
- fixed distribution of neuron **intrinsic dynamics**
1/3 Q, 1/3 B, 1/3 T (E_L varied)
- variety of **connection architectures** with fixed total number of links (same total g_{syn} for each neuron)
 - nearest neighbor (1-d and 2-d)
 - scale-free
 - random
 - **Hartelt**
 - small world (1-d and 2-d)
- varied **cell-type hierarchies**: placement of particular types of intrinsic dynamics within each network, based on ***betweenness centrality***
random, TBQ, TQB, BTQ, BQT, QTB, QBT

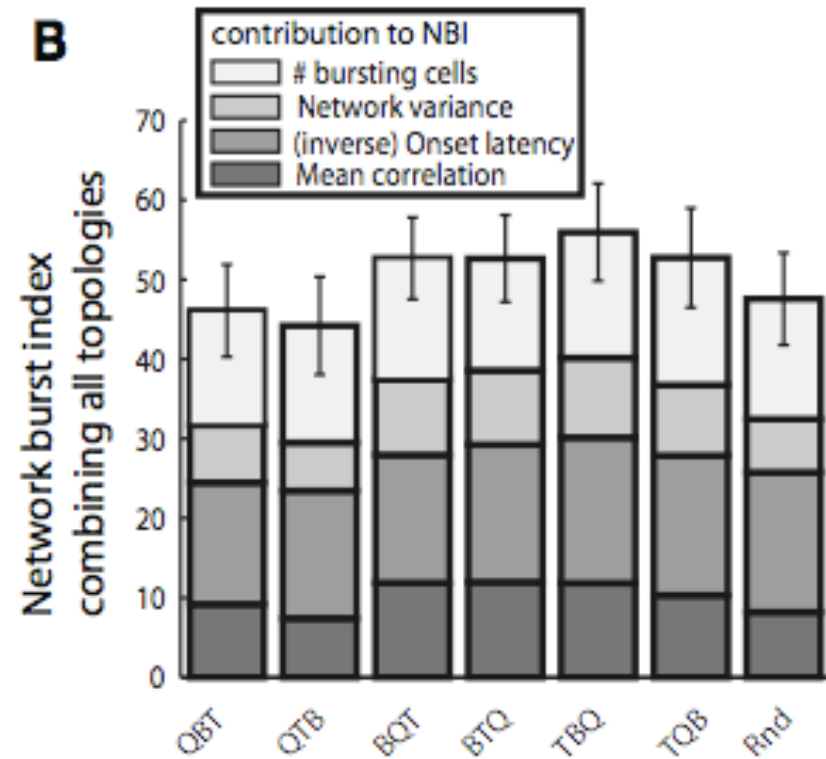


results: network burst synchrony vs. cell-type hierarchy

network burst synchrony is generally less sensitive to which cell type goes where than to network topology, esp. for strong synapses (exception: scale-free networks)



NBI vs. architecture



NBI vs. cell-type hierarchy